Original Research Article **Medicinal chemistry**

International Journal of Life science and Pharma Research

ISSN 2250-0480

STRUCTURAL VERIFICATION, MOLECULAR DOCKING AND ANTIPROLIFERATIVE ACTIVITY FOR AMINO ACETYLENIC OXY QUINOXALINES

ZUHAIR A MUHI-ELDEEN[1*], BAKR S MUSTAFA[1], ELHAM N AL-KAISSI[2] AND MOHAMMAD A GHATTAS[3]

[1]*Department of Medicinal Chemistry and Pharmacognosy, Faculty of Pharmacy, University of Petra, Amman, Jordan.*
[2] *Department of Pharmaceutics and Pharmaceutical Technology, Faculty of Pharmacy, University of Petra, Amman, Jordan.*
[3] *College of Pharmacy, Al Ain University of Science and Technology, Al Ain, United Arab Emirates*

ABSTRACT

Tyrosine kinase inhibitors of the epidermal growth factor receptor (EGFR) are of interest to drug companies. These proteins kinase (PKs) are considered as validated drug targets. In cancer, proteins kinases play a key role in regulating numerous cellular functions including increased proliferation, decreased apoptosis, increased invasion, metastasis, and promote angiogenesis. Tyrosine kinase overproduction inhibits the activity of various anticancer agents via suppression of key apoptotic mechanisms thereby leading to the development of cellular drug resistance. Targeting and inhibiting these kinases enzymes became attractive candidates for cancer therapy. The targeting of human epidermal growth factor receptor 2 (HER2 or ErB-2/neu) and epidermal growth factor receptor (EGFR or HER1/ErB1) by tyrosine kinase inhibitors (TKIs) represent a promising therapeutic approach in cancer therapy. The new novel 2- [4-(t-amino-1-yl)but-2-yn-1-yl]quinoxaline (ZB-2 to ZB-8), provide effective overlap with (EGFR or HER2) through ionic, hydrogen bonding, charge transfer and hydrophobicity. The introduction of different basic amino moiety with acetylenic group in signal transduction inhibitor represents a novel and new approach in the management and treatment of cancer. These speculations were supported by molecular docking and pharmacological activity which shows an effective overlap with EGFR to initiate the inhibition activity leading to cancer treatment.

KEYWORDS: ***Quinoxalinol; Amino acetylenic; Mannich reaction***

ZUHAIR A MUHI-ELDEEN*

Department of Medicinal Chemistry and pharmacognosy, Faculty of pharmacy, Univer sity of Petra, Amman, Jordan.

Received on: 14-02-2019
Revised and Accepted on: 27.05.2019
DOI: http://dx.doi.org/10.22376/ijpbs/lpr.2019.9.3.P1-12

INTRODUCTION

As the first protein kinase inhibitor to reach the market, imatinibe (Glevec or Gleevec) represents a milestone in anticancer therapy. It was also the first drug to target a molecular structure. It acts as a selective inhibitor for a hybrid kinase called Ber-Ab1 which is active in certain tumor cells. The tyrosine kinase active site residue on the Ab1 portion of the hybrid protein.[1] Gefitinib was developed by AstraZeneca and belongs to a group of structures known as the 4-anilinoquinazolines (Figure 1).[2] Gefitinib was found to mimic ATP and bind to the ATP-binding region of the kinase active site.[2-4] The binding of ATP itself involves two important hydrogen bonding interactions between the purine base of ATP and the protein backbone between amino acids Gln-767 and Met-769. One of these interactions involves the purine group acting as a hydrogen bond donor, while the other involves purine acting as a hydrogen bond acceptor. Gefitinib has two nitrogen atoms in the quinazoline ring and both act as hydrogen bond acceptors. Acquired resistance to Imatinib (Figure 2) has been observed due to mutations in the Ab1 kinase domain that prevents the drug from binding. Other inhibitors of the Abelson tyrosine kinase may include Lapatinib, Nilotinib, Dasatinib and Bosutinib. Lapatinib (Figure 3) was approved in March 2007, and it was the same quinazoline core as Gefitinib. It binds to an inactive form of the kinase which exposed a hydrophobic pocket that is not exposed in the active form. It has a fluorobenzyloxy substituent that form extra interaction with hydrophobic pocket, which results in a potent activity for an additional inhibition of other kinase called Erb-B2. So it is a dual-action inhibitor which can be used for those cancers that overepress both EGFR and ErbB2.[5] In reviewed various structural features of different compounds in use or under investigation as EGFR inhibitors, and considering the privilege group or considering the fractional base analysis in drug design and to reduce resistance. We investigated the synthesis of 2-quinoxalinol derivatives as new novel compounds presumably inhibit EGFR for the following reasons; 2-quinoxalinol as a structural analogue to quinazoline that is found in many EGFR inhibitors as seen in Gefitinib, Erlotinib and others. This isosteric isomer may provide better direction for binding to EGFR than previously synthesis compounds, and reducing resistance, aminoacetylenic moiety is a unique group that provide the appropriate functional groups to interact with EGFR through the basic amino group that is required for ionic bonding with the corresponding groups on EGFR receptor to induce the blockade activity, 2-butyne to provide the appropriate distance between the nitrogen of cyclicamine and 2-quinoxalinol. A quinoxalin initiate π-overlap with the ATP binding site in EGFR. These chemical interactions may generate new and effective signal transduction inhibitors of EGFR receptors, these interactions supported by molecular docking and pharmacological investigation.

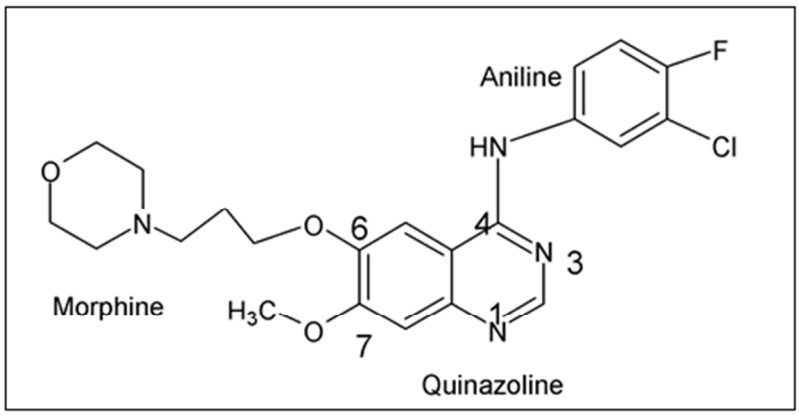

Figure 1

N-(3-chloro-4-fluoro-phenyl)-7-methoxy-6-(3-morphine-4-yl-propoxy)quinazoline-4-amine Gefitinib).[3]

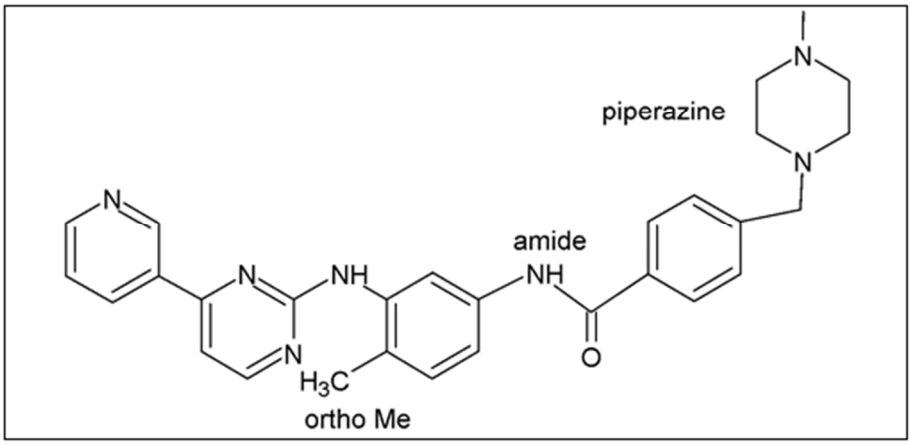

Figure 2
4-[(4-methylpiperazin-1-yl)methyl]-n-[4-methyl-3-(4-pyridine-3-ylpyridin-2-l)amino]phenylbenzamide (Imatinib).

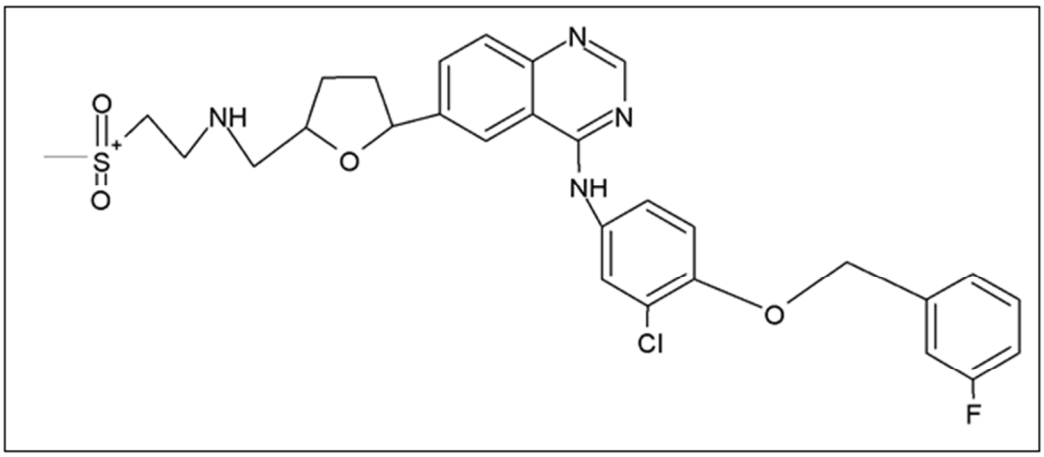

Figure 3
Lapatinib (Tyverb)

MATERIALS AND METHODS

Chemicals

The following chemicals were used: 2-quinoxalinol, propargyl bromide, 2-methylpiperidine 99%, hexamethyleneimine 98%, 2,6-dimethylpiperidine, pyrrolidine 98%, N-methylpiperazine 99%, morphine 99% (all of these chemicals were purchased from Sigma-Aldrich USA), peroxide-free 1,4-dioxan (Full Time China), acetonitrile 99.7% (PanReAc Química SA, EU), paraformaldehyde (BDH chemicals Ltd Poole, England), cuprous chloride (East Anglia Chemicals Hadleigh Ipswich), chloroform (TEDIA, USA), potassium carbonate anhydrous pure (Gainland Chemical Company (GCC), UK), deuterated dimethyl sulfoxide (DMSO) (BBC Chemicals for lab, EU), (3-(4,5-dimethylthiazol-2-yl)-2,5-diphenyltetrazolium bromide) MTT(Dorset, UK).

Instruments

Infrared spectra (IR) were recorded using FTIR spectrophotometer of Ray Leigh WQF-520A FTIR by Beijing Rayleigh analytical instrument Co LTD, Rotary evaporator of Stuart by Bibby Scientific Limited Store, differential scanning calorimeter of Mettler Toledo DSC 1 Star system, H1 and C13 NMR were acquired with the aid of Varian 300 MHz spectrometer and DMSO-d6 as solvent, and TMS as standard. The analysis was carried out Euro EA elemental analyzer. The maximum deviation of the result obtained were (+2.59 to -2.95) from the theoretical value, which is considered within the acceptable variation range in results (±0.4%) according to the accuracy of Euro EA elemental analyzer (Jordan University).

Molecular docking

In this docking study the EGFR-kinase domain used was downloaded from the protein data bank (PDB:1XKK)[6] and the co-crystallized ligand and

all water molecules were removed from the protein structure. The protein structure was checked by MOE using the protein preparation module. Then, it was processed by the Protein Preparation Wizard in the Maestro software to set up partial charges on each atom and protonation states on each ionizable group.[7,8] ATP binding site of the EGFR kinase domain was identified by its own co-crystallized ligand (lapatinib) then a grid box of a 60 x 50 x 60 Å size was created using the Receptor Grid Generation module in Glide [9,10] ; with a grid spacing of 0.375 Å. The hydroxyl and thiol groups present in the active site were set as rotatable. Ligands 3D were prepared using the LigPrep module in the Maestro program.[11] Two ionization states were generated for the tertiary amine groups and all chiral possibilities were enumerated. Next, ligands were docked into the ATP binding site using the Glide software, where the extra-precision (XP) Algorithm was employed for the conformational sampling process. Subsequently, docked poses were scored via the Glide_XP scoring function which includes terms for van der Waals, hydrogen bond, electrostatic interactions, desolvation penalty and penalty for intra-ligand contact. A hydrogen bonding strain was set up on the Met793 backbone amine group in the hinge region to attract the binding of a ligand hydrogen bond acceptor. Such a constraint has proven to significantly improve the docking of kinase inhibitors in the ATP-binding site.

Assay of antiproliferative activity

Cell lines and culture condition

The human breast adenocarcinoma MCF-7 and the human colon cancer Caco-II cell lines were used and were purchased from the American Type Culture Collection (Rockville, MD, USA). The cells were grown and maintained in Dulbecco's modified Eagle's medium (DMEM, Gibco, Waltham, MD, USA) supplemented with 1% of 2 mM L-glutamine (Lonza), 10% fetal calf serum (Gibco, Paisley, UK), 50 IU/ml penicillin/streptomycin (Sigma, St. Louis, MO) and amphotericin B (Sigma, St. Louis, MO) and were incubated at 37°C in humidified atmosphere of 95% O_2 and 5% CO_2. Cell cultures were passaged every 2-3 days or whenever the cells were reaching 80% confluent. Cells were seeded at density of 6-8 x 10^3 cells/well in 96-well microplates in appropriate medium and incubated at 37°C for 24 h to allow for adhesion.

Cell proliferation assay (MTT)

To evaluate cell proliferation, the MTT colorimetric assay was used as previously described.[12] The MTT [3-(4,5-dimethylthiazol-2-yl)-2,5-diphenyltetrazolium bromide] dye reduction assay works on the principle that mitochondrial succinate tetrazolium reductase system converts the yellow colored MTT into its purple formazan derivative.[13] The amount of dye produced is proportional to the number of live cells. The newly synthesized compound (ZB2-ZB8) at the desirable concentration were added to the wells. After the end of the exposure period (48 h), the medium was removed and 50 µl MTT solution was added to each well and incubated for 4 h at 37°C with mild shaking. The yellow tetrazolium dye of MTT was reduced by metabolically active cells into an intracellular purple formazan product. Afterward, DMSO was added to each well to solubilize the purple formazan crystals formed. Then the absorbance was read using a microplate enzyme-linked immunosorbent assay (ELISA) reader at 570 nm filter. Survival rates of the controls were set to represent 100% viability. Untreated cultures were used as controls groups. Doxorubicin was used as the positive control and 0.1% DMSO in DMEM media as a solvent control.

Chemistry

Synthesis

2-(prop-2-yn-1-yloxy)quinoxaline (ZB-1)

A mixture of 2-quinoxalinol (1.6 g 0.01 mol) and K_2CO_3 (2 g 0.02 mol) as a catalytic base in acetonitrile (30 ml), was refluxed up to 68-72°C for 1 h.3-bromo-1-propyne (3 g 0.02mol) was added at 70°C drop wise to the above solution for 15 min. The mixture was stirred for 45 min. after cooling, the insoluble residue was removed by filtration to give yellowish solution. The filtrate concentrated under reduced pressure yielding yellow powder compound (ZB-1) which is the alkylated ZB-1 (Figure 4). The physical, chemical and instrumental data are listed under results. The IR spectra of 2-(prop-2-yn-1-yl)-quinoxaline (ZB-1) showed the terminal acetylenic proton at (3330 cm^{-1}), acetylenic C≡C at 2200-2114 cm^{-1} the aryl double bond stretch at 1550-1439 cm^{-1} and the aliphatic carbon at 1400 cm^{-1} and 2817 cm^{-1}.

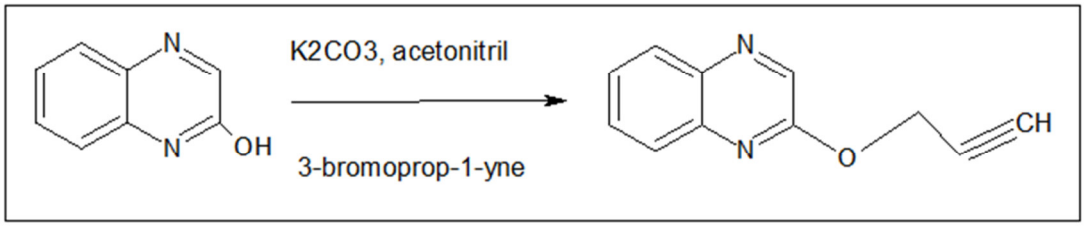

Figure 4.
2-(prop-2-yn-1-yloxy)quinoxaline (ZB-1)

2-[4-(t-amino-1-yl)but-2-yn-1-yl]oxy quinoxaline (ZB-2 to ZB-8)

A mixture of 2(prop-2 yn-1-yloxy)quinoxaline (ZB-1) (0.5 g 0.002 mol), paraformaldehyde(0.1 g 0.002 mol), cyclic amine around (0.4 ml), catalytic amount of cuprous chloride (0.03 mol) in peroxide-free dioxane (45 ml) was left, with magnetic stirring for 60 min at 70-75°C. After cooling, the insoluble residue was removed by filtration, and the filtrate was concentrated under reduced pressure to afford the desired brown powder compounds, ZB-2 to ZB-8. All compounds crystallized from 70-80% ethanol/water.

STATISTICAL ANALYSIS

The data obtained were analyzed using statistical packages (SPSS) for social science software. The data were presented as mean ± SD. Probability value (P) of less than 0.05 was considered statistically significant

RESULTS

2-(prop-2-yn-1-yloxy)quinoxaline (ZB-1)

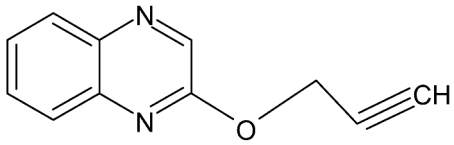

Powder Yield	1.2 g (97.1%)
Melting point	158.5-160.0°C
DSC point	158.83°C

IR: 735-548 (Ar-C=C, bending), 1163-912 (Ar-C=C, bending), 1439 (Ar, stretch), 1645 (C-O, stretch), 2114 (C≡C, stretch), 3180 (Ar-H, stretch). ^{1}H-NMR (DMSO-d6): δ 3.33 (s, 1H, C≡CH), 5.03 (d, 2H, O-CH_2-C≡), 7.36-8.30 (m, Ar-H), of quinoxaline ^{13}C-NMR (DMSO-d6): δ 40.00 (s, 1C, ≡CH), 75 (s, 1C, O-CH_2), 78 (s, 1C, O-CH_2-C≡), 118-150 (m, Ar-C). Anal. Calcd, ($C_{11}H_8N_2O$): C (81.4 %); H (4.9 %); N (8.6 %). Found C (81.13%); H (4.52 %); N (8.22 %).

2-[(4-(4-methylpiperazin-1-yl)but-2-yn-1-yl)oxy]quinoxaline (ZB-2)

ZB-2 compound was prepared following the general procedure for synthesis of (ZB-2 to ZB-8)

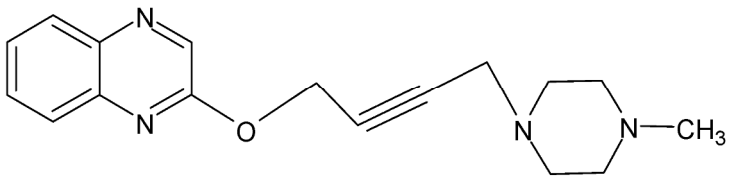

Powder Yield	2 g (67.5%)
Melting point	248.9°C
DSC point	250.34°C

IR: 853-659 (Ar C=C, bending), 1290-970 (Ar C=C, bending), 1470 (Ar C=C, stretch), 1553-1470 (Ar C=C, stretch),1600 (C-O, stretch), 2320 (C≡C, stretch), 2900 (≡CH, stretch). ^{1}H-NMR (DMSO-d6): δ 0.8-2.1 (8H, multiplet), 2.46 (s, 4H, N-CH_3), 3.8 (s, CH_2-O-Ar), 7.8 (multiplet, 6H, Ar-H), of quinoxaline ^{13}C-NMR (DMSO-d6): δ 40.00 (s, 1C, ≡CH), 75 (s, 1C, O-CH_2-C≡), 78 (s, 1C, O-CH_2-C≡), 118-150 (m, Ar-C). Anal. Calcd, ($C_{17}H_{20}N_4O$): C (78.4 %); H (7.69 %); N (10.76 %). Found C (78.61%); H (7.65 %); N (10.45 %).

2-[(4-(2,6-dimethyl piperidin-1-yl)but-2-yn-1-yl)oxy]quinoxaline (ZB-3)

ZB-3 compound was prepared following the general procedure for synthesis of (Z-2 to ZB-8) compounds.

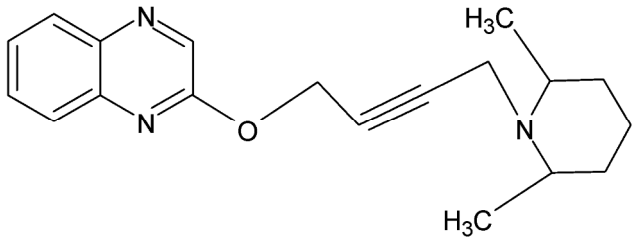

Powder Yield	1.8 g (58.6%)
Melting point	149.2°C
DSC point	150.44°C

IR: 754-498 (Ar C=C, bending), 1227-962 (Ar C=C, bending), 1439, 1415, 1302 (Ar C=C, stretch), 1660 (C-O, stretch), 2351 (C≡C, stretch), 2933, 2819 (Ar-H, stretch), ^{1}H-NMR (DMSO-d6): δ 0.8-0.83 (d, 3H, C-CH_3), 1.03-1.05 (d, 3H, C-CH3) 1.33-1.44 (d, 1H, C≡C-CH_2-N), 2.13-2.46 (6H of the cyclic amine), 3.34 (t, 2H, C≡C-CH_2-N),5.06-5.14(d, 2H, O-CH2-C≡), 7.22-8.24 (m, 5H, Ar-H),of quinoxaline ^{13}C-NMR (DMSO-d6): δ 40.00 (s, 1C, ≡CH), 75 (s, 1C, O-CH_2-C≡), 78 (s, 1C, O-CH_2-C≡), 118-150 (m, Ar-C). Anal. Calcd, ($C_{19}H_{23}N_3O$): C (81.40 %); H (8.21%); N (7.50 %). Found C (81.20 %); H (7.95%); N (7.33%).

2-[(4-(2-methylpiperidin-1-yl)but-2-yn-1-yl)oxy]quinoxaline (ZB-4)

ZB-4 was prepared following the general procedure for synthesis of (ZB-2 to ZB-8) compouns.

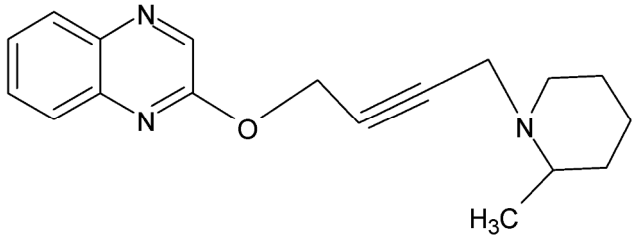

Powder Yield	2.2 g (58.6%)
Melting point	130.2°C
DSC point	131.39°C

IR: 814-600 (Ar C=C, bending), 1176-1124 (Ar C=C, bending), 1500-1308 (Ar C=C, stretch), 1649 (C-O, stretch), 2333 (C≡C, stretch), 2933, 2802 (Ar-H, stretch).^{1}H-NMR (DMSO-d6): δ 2.46-2.50 (d, 3H, C-CH_3), 2.13-2.46 (6H of the cyclic amine) 0.79-1.51 (d, 3H, C-CH3) 3.12-3.52 (m, 2H, C≡C-CH_2-N), 5.06 (s, 2H, O-CH2-C≡), 7.23-8.24 (m, 5H, Ar-H), of quinoxaline ^{13}C-NMR (DMSO-d6): δ 40.00 (s, 1C, ≡CH), 75 (s, 1C, O-CH_2-C≡), 78 (s, 1C, O-CH_2-C≡), 118-150 (m, Ar-C). Anal. Calcd, ($C_{18}H_{21}N_3O$): C (81.20 %); H (7.89%); N (7.89 %). Found C (81.51 %); H (7.91%); N (7.88%).

2-[(4-(pyrrolidin-1-yl)but-2-yn-1-yl)oxy]quinoxaline (ZB-5)

ZB-5 compound was prepared following the general procedure for synthesis of (ZB-2 to ZB-8) compounds.

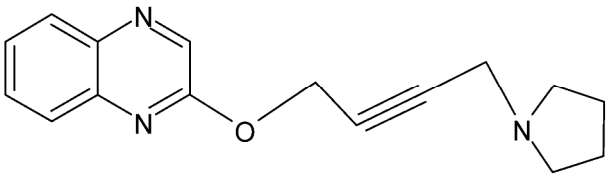

Powder Yield	1.1 g (58.6%)
Melting point	233.11°C
DSC point	234.14°C

IR: 754-639 (Ar C=C, bending), 1126-906 (Ar C=C, bending), 1549-1306 (Ar C=C, stretch), 1670 (C-O, stretch), 2374 (C≡C, stretch), 2954, 2816 (Ar-H, stretch)**.**[1] H-NMR (DMSO-d6): δ 1.06-2.14 (m, 8H of the cyclic amine), 3.23-3.41 (d, 2H, C≡C-CH_2-N), 5.10-5.21(s, 2H, O-CH2-C≡), 7.12-8.25 (m, 5H, Ar-H), of quinoxaline ^{13}C-NMR (DMSO-d6): δ 40.00 (s, 1C, ≡CH), 75 (s, 1C, O-CH_2-C≡), 78 (s, 1C, O-CH_2-C≡), 118-150 (m, Ar-C). Anal. Calcd, ($C_{16}H_{17}N_3O$): C (80.67 %); H (7.14%); N (8.82%). Found C (80.45%); H (7.04%); N (8.77%)**.**

4-[(4-(quinoxaline-2-yloxy)but-2-yn-1-yl)morphine (ZB-6)

ZB-6 compound was prepared following the general procedure for synthesis of (**ZB-2 to ZB-8**) compounds.

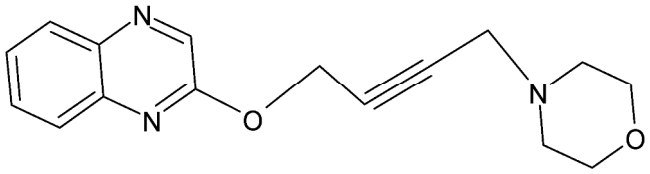

Powder Yield	2.5 g (58.6%)
Melting point	240.11°C
DSC point	240.45°C

IR: 2954, 2827 (acetylenic ≡CH, stretch), 2376 (C≡C, stretch), 1660 (C=O, stretch), 1543-1254 (Ar C=C, stretch), 1124-891 (Ar C=C, bending), 792-643 (Ar C=C, bending). ^{1}H-NMR (DMSO-d6): δ 1.06-2.14 (m, 8H of the cyclic amine), 3.23-3.41 (d, 2H, C≡C-CH_2-N), 5.10-5.21(s, 2H, O-CH2-C≡), 7.12-8.25 (m, 5H, Ar-H), of quinoxaline ^{13}C-NMR (DMSO-d6): δ 39.19-40.83 (m, carbon of cyclic amine), 40 (m, C≡C-CH_2-N), 45 (m, H3C-O-CH_3), 115 (s, O-CH_2-C≡), 120 (s, O-CH_2-C≡) 125-155 (m, Ar-C). Anal. Calcd, ($C_{16}H_{17}N_3O$): C (73.01%); H (6.91%); N (8.53%). Found C (73.40%); H (6.87%); N (8.46%)**.** IR: 792-643 (Ar C=C, bending), 1124-891 (Ar C=C, bending), 1543-1254 (Ar C=C, stretch), 1660 (C-O, stretch), 2376 (C≡C, stretch), 2954, 2827 (Ar-H, stretch)**.**[1]H-NMR (DMSO-d6): δ 1.06-2.14 (m, 8H of the cyclic amine), 3.23-3.41 (d, 2H, C≡C-CH_2-N), 5.10-5.21(s, 2H, O-CH2-C≡), 7.12-8.25 (m, 5H, Ar-H), of quinoxaline ^{13}C-NMR (DMSO-d6): δ 39.19-40.83 (m, carbon of cyclic amine), 40 (m, C≡C-CH_2-N), 45 (m, H3C-O-CH_3), 115 (s, O-CH_2-C≡), 120 (s, O-CH_2-C≡) 125-155 (m, Ar-C). Anal. Calcd, ($C_{16}H_{17}N_3O$): C (73.01%); H (6.91%); N (8.53%). Found C (73.40%); H (6.87%); N (8.46%)**.**

2-[(4-(hexamethylenediamine-1-yl)but-2-yn-1-yl)oxy]quinoxaline (ZB-7)

ZB-7 compound was prepared following the procedure for synthesis of (**ZB-2 to ZB-8**) compounds.

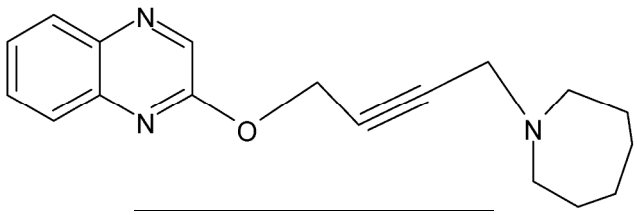

Powder Yield	1.2 g (40.6%)
Melting point	258.9°C
DSC point	260.86°C

IR: 887-667 (Ar C=C, bending), 1255-935 (Ar C=C, bending), 1547, 1227, 1389 (Ar C=C, stretch), 1691 (C-O, stretch), 2337 (C≡C, stretch), 2954, 2817 (Ar-H, stretch).^{1}H-NMR (DMSO-d6): δ 1.4-1.70 (m, 12H of the cyclic amin), 2.46-2.53 (s, C≡C-CH_2-N), 3.37-3.38 (d, 2H, O-CH_2- C≡), 7.19-8.19 (m, 5H, Ar-H), of quinoxaline ^{13}C-NMR (DMSO-d6): δ 39.19-40.83 (m, carbon of cyclic amine), 40 (m, C≡C-CH_2-N), 45 (m, H3C-O-CH_3), 115 (s, O-CH_2-C≡), 120 (s, O-CH_2-C≡) 125-155 (m, Ar-C). Anal. Calcd, ($C_{18}H_{21}N_3O$): C (81.20 %); H (7.89%); N (7.89 %). Found C (81.51%); H (7.86%); N (7.93%).

2-[(4-(piperidin-1-yl)but-2-yn-1-yl)oxy]quinoxaline (ZB-8)

ZB-8 compound was prepared following the general procedure for synthesis (**ZB-2 to ZB-8**) compounds.

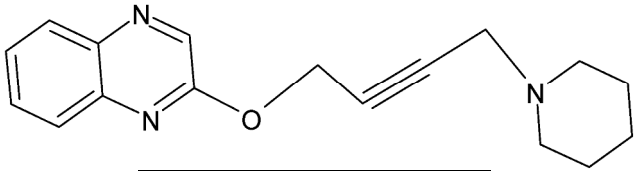

Powder Yield	1.5 g (53.3%)
Melting point	123.27°C
DSC point	124.88°C

IR: 806-624 (Ar C=C, bending), 1097-979 (Ar C=C, bending), 1541-1376 (Ar C=C, stretch), 1617 (C-O, stretch), 2245 (C≡C, stretch), 2924, 2863 (Ar-H, stretch).^{1}H-NMR (DMSO-d6): δ 0.8-1.86 (m, 10H of the cyclic amin), 3.42 (s, 2H, CH_2-N), 4.48 (s, 2H, Ar-OCH_2)7.20-8.15 (m, 5H, Ar-H), of quinoxaline ^{13}C-NMR (DMSO-d6): δ 39.19-40.83 (m, carbon of cyclic amine), 40 (m, C≡C-CH_2-N), 45 (m, H3C-O-CH_3), 115 (s, O-CH_2-C≡), 120 (s, O-CH_2-C≡) 125-155 (m, Ar-C). Anal. Calcd, ($C_{17}H_{19}N_3O$): C (80.95 %); H (7.53%); N (8.33 %). Found C (80.91%); H (7.23%); N (8.36%).

DISCUSSION

The designed compounds were prepared according to schemes 1 and 2, the synthesis of ZB-1 was generated through nucleophilic displacement of the bromine atom located at 3-bromoprop-1-yne. 2-(prop-2-yn-1-yloxy)quinoxaline (ZB-1) with paraformaldehyde, appropriate cyclic amine and catalytic amount of cuprous chloride in Mannich reaction yielded the desired compounds (ZB-2 to ZB-8). Through IR, ^{1}H-NMR, ^{13}C-NMR and elemental analysis the structures were verified as shown in the results. The mannich reaction proposed mechanism is described in scheme 2. In order to proceed the mannich reaction, a reactive immonium cations intermediates should yield from the condensation of formaldehyde and appropriate cyclicamine (Schiff base formation). The desired mannich products (ZB-2 to ZB-8) was generated from the attack of the carbanion in 2-(prop-2-yn-1-yloxy)quinoxaline cuprous salt on the Schiff base.

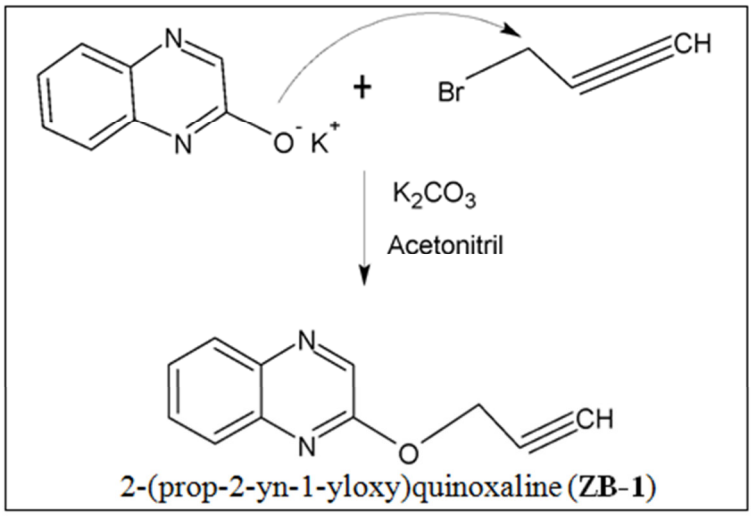

Scheme 1
alkylation reaction of 2-(prop-2-yn-1-yloxy)quinoxaline (ZB-1)

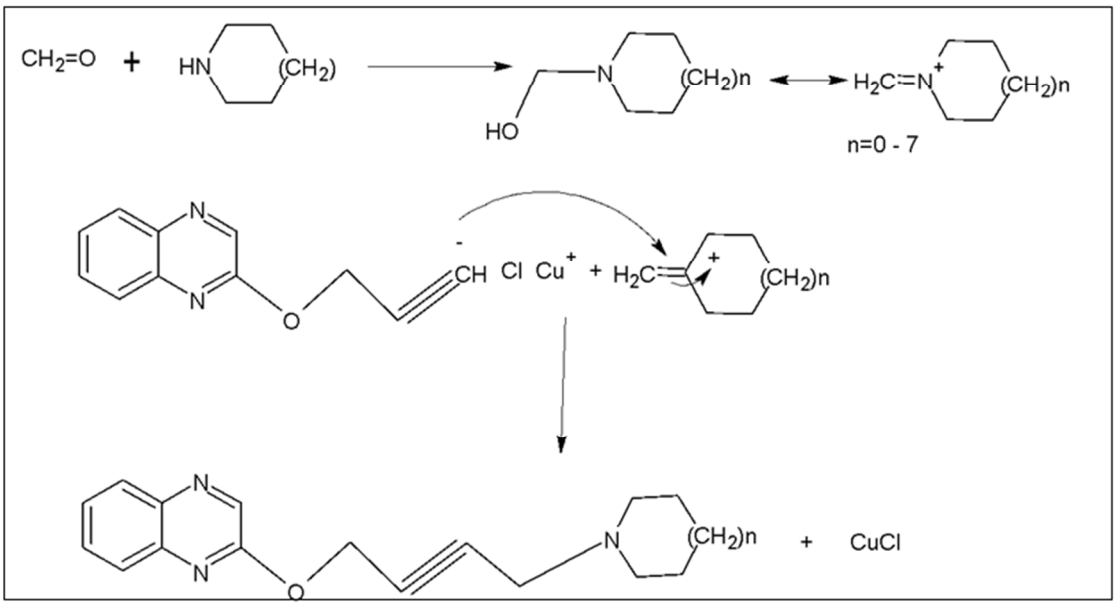

Scheme 2
Proposed mannich reaction

The design of these compounds as epidermal growth factor receptor antagonists was based on rationalization of the important criteria required to overlap effectively with EGFR to induce antagonistic activity. A basic cyclic amine group for ionic interaction or hydrogen bonding, the acetylenic group for electrostatic interaction, the 2-butyne provides the appropriate distance between the basic nitrogen and quinoxaline as a fractional base approach to quinazoline ring found in many effective EGFR antagonists. The results of molecular docking supported our assumption in the design of new novel EGFR antagonist. Kinases inhibitors are usually having a hydrophobic cyclic system that fits in a hydrophobic specificity pocket on the other side of the binding site.[14] They are known to have a cyclic system which has a nitrogen atom that is able to make hydrogen bonding with the backbone of the ATP-binding site hinge region.[15, 16] Accordingly, our compounds were designed to have a two heterocyclic system linked with each other via butynyl spacer. Such a design provides the ability to bind with the purine binding region via the first cyclic system and with the second binding region via the amino cyclic group through H-bonding or anionic 2-butyne, electrostatic and hydrophobic binding.[17] Docking our compounds along with the co-crystallized ligand, lapatinib, into the ATP-binding site of the EGFR kinase domain has resulted in energetically favorable binding modes. As shown in table 1, compound ZB-8 (Glide_XP score = -9.4 kcal/mol) has a lowest docking score amongst the quinoxaline–based compounds, the famous EGFR-kinase inhibitor lapatinib was able to score the lowest binding energy (Glide_XP score = -13.7 kcal/mol). However, taking into consideration the docking score with the ligand size, all the four compounds where docked had a better ligand efficiency (ligand efficiency > -0.40 kcal/mol) in comparison with lapatinib (ligand efficiency = -0.34 kcal/mol) (except ZB-3), this showed that our compounds (ZB-5, ZB-4, ZB-8) with ligand efficiency better than Lapatinib (-0.4, -0.3 respectively) and these compounds can be good candidate as EGFR kinase lead compounds generated from this research. Looking at the docking binding mode of ZB-8 (Figure. 5), the nitrogen in the quinoxaline ring was able to make the usual hydrogen bond with the backbone amide of the hinge region (as Met793). Interestingly, the other part of ZB-8, the piperidine ring was placed on at the hydrophobic specificity pocket, making van der Waals interactions with the surrounding residues in addition to an interesting hydrogen bonding interaction with the Thr854 side chain. To sum up, these compounds appear to have what it takes to be good and promising leading compounds for the EGFR-kinase enzyme. Considering their small size and the important features they have in common with the standard kinase inhibitor (example lapatinib). Pyrrolidine cyclic amine ZB-5 generated good binding energy, increase the size to six membered ring increase the flexibility to provide the best overlaps shown in ZB-8, static factor around the basic nitrogen as ZB-3 provide the lowest binding energy relative to the other ZB-5, ZB-4 and ZB-8.

Table 1
Binding energies of our docked compounds into the EGFR kinase ATP-binding site

Molecule	Structure	Glide_XP score (kcal/mol)	Ligand efficiency (kcal/mol)
Lapatinib	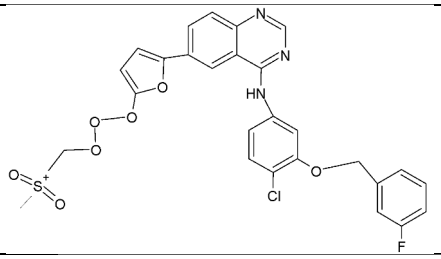	-13.7	-0.34
	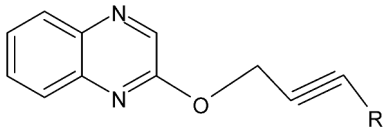		
ZB-5	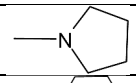	-8.8	-0.44
ZB-4	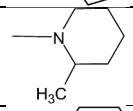	-9.2	-0.42
ZB-8	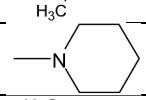	-9.4	0.45
ZB-3	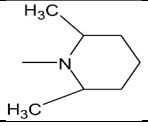	-5.9	-.26

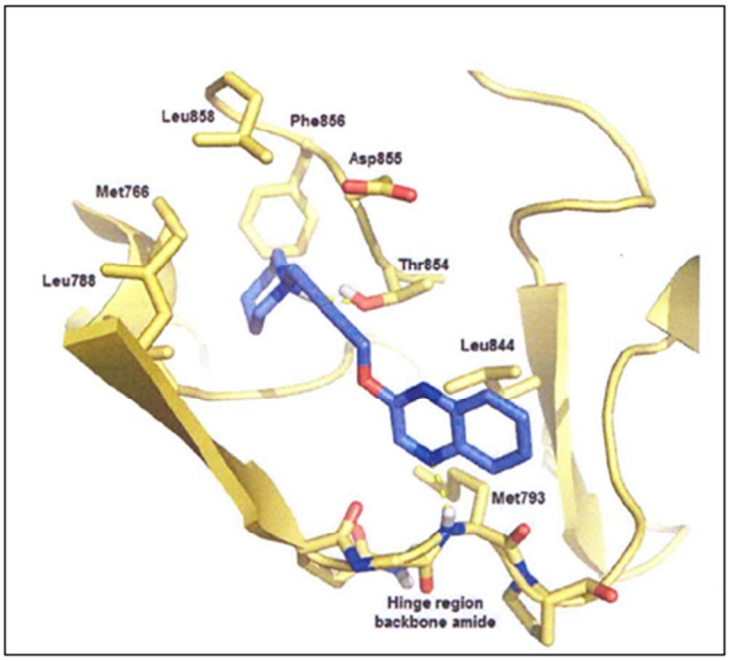

Figure 5
Shows the binding mode demonstrated by ZB-8 (blue) in the ATP-binding site of the EGFR kinase domain (gold). The figure was generated by PyMol.[20] Hydrogen bonding is shown as yellow dotted line. Some protein chains are not shown for clarity.

The antiproliferative activities for the synthesized compounds (ZB-2 to ZB-8) The newly synthesized amino acetylenic quinoxaline derivatives were tested against breast (MCF-7) and colon cancer lines (Caco-2) for their antitumor activities.[18, 19] Interestingly, these compounds exhibited some antiproliferative activities relative to known standard doxorubicin that has IC_{50} values of 2-10 µM/L (table 2). Further structural modification should enhance the antiproliferative activities.

Table 2
The IC50 values (µM/L) of the examined compounds relative to the standard doxorubicin with IC-50 of 10 µM/L.

Compound	µM/L	
	MCF-7 x 10^{-6}	Caco-2 x 10^{-6}
ZB-1	2.23 ± 0.02	2.87 ± 0.01
Zb-3	2.26 ± 0.01	2.28 ± 0.03
ZB-4	1.65 ± 0.05	1.70 ± 0.02
ZB-6	1.80 ± 0.03	2.15 ± 0.02
Doxorubicin	2-10	2-10

Values are mean ±SD; (n=3).
Abbreviation IC50: inhibitory concentration of 50% of the sample

CONCLUSION

The synthesis and characterization of the new series of 2-[(4-(amino-1-yl)but-2-yn-1-yl)oxy]quinoxaline (ZB-2 to ZB-8) were accomplished through the alkalyated of quinoxalinol. The reaction of alkylated quinoxaline under mannich condition were generated for the desired compounds. The modes of interaction with the EGFR. Particularly, they overlap with the ATP binding domain in the kinase moiety in EGFR by hydrogen and ionic bonding with Met793 and Thr854 amino acids leading to the blockade of the receptor. The unique introduction of aminoacetylenic moiety reproduces a novel approach in synthesizing new EGFR inhibitors different from other products in use Gefitinib, Erlotinib, and lapatinib. Molecular docking of the 2-[(4-(amino-1-yl)but-2-yn-1-yl)oxy]quinoxaline (ZB-2 to ZB-8) compounds supported this speculations and showed a promising approach in management of cancer provided by these new compounds (Zb-2 to ZB-8) promoted our interest to carry out further structure modifications by addition of lipophilic group as alkylox, halogen, aryl group will be taking in consideration.

AUTHOR CONTRIBUTION STATEMENT

Prof. Zuhair Muhi-eldeen conceived and conducted the design of the molecules and supervise the chemical reactions, Prof. Elham Al-Kaissi wrote and analyzed the data, Dr. Mohammad Ghattas carried out the molecular docking and analysed the data, Dr. Bakr Khalil carried out the chemical reaction and provided the anti-proliferative data.

ACKNOWLEDGMENT

This work was done and funded by faculty of Pharmacy / University of Petra, Amman, Jordan.

CONFLICT OF INTEREST

Conflict of interest declared none.

REFERENCES

1. Capdeville R, Buchdunger E, Zimmermann J, Matter A. Glivec (STI571, imatinib), a rationally developed, targeted anticancer drug. Nat Rev Drug Discov . 2002;1(7):493–502. DOI:10.1038/nrd839
2. Nguyen K-SH, Kobayashi S, Costa DB. Acquired Resistance to Epidermal Growth Factor Receptor Tyrosine Kinase Inhibitors in Non–Small-Cell Lung Cancers Dependent on the Epidermal Growth Factor Receptor Pathway. Clin Lung Cancer . 2009;10(4):281–9. DOI:10.3816/clc.2009.n.039
3. Abouzid K, Shouman S. Design, synthesis and in vitro antitumor activity of 4-aminoquinoline and 4-aminoquinazoline derivatives targeting EGFR tyrosine kinase. Bioorg Med Chem . 2008;16(16):7543–51. DOI:10.1016/j.bmc.2008.07.038

4. Jemal A, Siegel R, Ward E, Hao Y, Xu J, Murray T, et al. Cancer Statistics, 2008. CA Cancer J Clin . 2008;58(2):71–96. DOI:10.3322/ca.2007.0010
5. Geyer CE, Forster J, Lindquist D, Chan S, Romieu CG, Pienkowski T, et al. Lapatinib plus Capecitabine for HER2-Positive Advanced Breast Cancer. N Engl J Med . 2006;355(26):2733–43. DOI:10.1056/nejmoa064320
6. Wood ER, Truesdale AT, McDonald OB, Yuan D, Hassell A, Dickerson SH, et al. A Unique Structure for Epidermal Growth Factor Receptor Bound to GW572016 (Lapatinib). Cancer Res . 2004;64(18):6652–9. DOI:10.1158/0008-5472.can-04-1168
7. Chemical Computing Group ULC, Molecular Operating Environment (MOE), 2013.08, Suite #910, 1010 Sherbrooke St. West, Montreal, QC, Canada, H3A 2R7, 2018. Available from: https://www.chemcomp.com
8. Schrödinger, LLC, Schrödinger Release 2015-1, Protein Preparation Wizard; epik, Schrödinger Suite, Impact version 6.7, New York, NY, 2015 https://www.schrodinger.com/epik. Available from: https://www.schrodinger.com/protein-preparation-wizard
9. Madhavi Sastry G, Adzhigirey M, Day T, Annabhimoju R, Sherman W. Protein and ligand preparation: parameters, protocols, and influence on virtual screening enrichments. J Comput Aided Mol Des . 2013;27(3):221–34. DOI:10.1007/s10822-013-9644-8
10. Brisson M. Discovery and Characterization of Novel Small Molecule Inhibitors of Human Cdc25B Dual Specificity Phosphatase. Mol Pharmacol . 2004;66(4):824–33. DOI:10.1124/mol.104.001784
11. Schrödinger, LLC, Small-Molecule Drug Discovery Suite 2019-1, Schrödinger, LLC, New York, NY, 2019. Available from: https://www.schrodinger.com/suites/small-molecule-drug-discovery-suite
12. Morris GM, Goodsell DS, Halliday RS, Huey R, Hart WE, Belew RK, et al. Automated docking using a Lamarckian genetic algorithm and an empirical binding free energy function. J Comput Chem. 1998;19(14):1639–62. DOI:10.1002/(sici)1096-987x(19981115)19:14%3C1639::aid-jcc10%3E3.0.co
13. Morris GM, Huey R, Lindstrom W, Sanner MF, Belew RK, Goodsell DS, et al. AutoDock4 and AutoDockTools4: Automated docking with selective receptor flexibility. J Comput Chem . 2009;30(16):2785–91. DOI:10.1002/jcc.21256
14. Schrödinger, LLC, Schrödinger Release 2015-1: LigPrep, Versatile generation of accurate 3D molecular models, New York, NY, 2015. Available from: https://www.schrodinger.com/ligprep
15. Friesner RA, Murphy RB, Repasky MP, Frye LL, Greenwood JR, Halgren TA, et al. Extra Precision Glide: Docking and Scoring Incorporating a Model of Hydrophobic Enclosure for Protein−Ligand Complexes. J Med Chem . 2006;49(21):6177–96. DOI:10.1021/jm051256o
16. Perola E. Minimizing false positives in kinase virtual screens. Proteins Struct Funct Bioinforma . 2006;64(2):422–35. DOI:10.1002/prot.21002
17. Muhi-eldeen ZA, Alani B, Al-kaissi EN, Bardaweel SK, Gattas M, Arafat T, et al. Synthesis , Structural Elucidation of Aminoacetylenicoxyquinazoline and their Antiproliferative Activities. 2017;9(23):38–45.
18. Bardaweel SK, Tawaha KA, Hudaib MM. Antioxidant, antimicrobial and antiproliferative activities of Anthemis palestina essential oil. BMC Complement Altern Med . 2014;14(1). DOI:10.1186/1472-6882-14-297
19. Siva priyadharshini SR, Padma PR. Kaempferol extracts differential effect on KB oral carcinoma cells and normal human buccal cells. Int J Pharma Bio Sci. 2016 Jul;7(3):1244-52.
20. Schrödinger, LLC, The PyMOL Molecular Graphics System, version 1.8, New York, NY, 2015. available from: https://pymol.org/2/support.html